

Diffusion-weighted MRI of kidney in the diagnosis of clear cell renal cell carcinoma of various grades of differentiation

Yulian Mytsyk¹, Ihor Dutka², Iryna Komnatska², Andrzej Górecki³, Borys Yuriy⁴, Iryna Shatynska-Mytsyk¹

¹ Diagnostic Imaging Department, National Medical University, L'viv, Ukraine

² Euroclinic Medical Centre, L'viv, Ukraine

³ ZOZ Nr. 2, Rzeszów, Poland

⁴ Department of Urology, National Medical University, L'viv, Ukraine

Mytsyk Y, Dutka I, Komnatska I, Górecki A, Yuriy B, Shatynska-Mytsyk I. Diffusion-weighted MRI of kidney in the diagnosis of clear cell renal cell carcinoma of various grades of differentiation. *J Pre-Clin Clin Res.* 2015; 9(1): 30–35. doi: 10.5604/18982395.1157573

Abstract

Introduction. Renal cell carcinoma (RCC) is the most common malignant epithelial tumour of the kidney, accounting for 85–90% of all solid renal tumours in adults and comprising 1–3% of all malignant visceral neoplasms. Recently, computed tomography (CT) has been considered the 'gold standard' in the diagnostic imaging of RCC; however, the use of CT is always associated with radiation exposure and consequently carries a significant increase in the risk of malignancy for patients with neoplastic processes. In recent years, magnetic resonance imaging (MRI) is increasingly attracting the attention of clinicians as the method of choice for the diagnosis and staging of RCC, due to several advantages over CT.

Materials and method. The study involved 62 adult patients with a pathologically verified clear cell subtype of the renal cell carcinoma (ccRCC) and 15 healthy volunteers. All patients underwent renal MRI which included diffusion-weighted imaging (DWI) with subsequent apparent diffusion coefficient (ADC) measurement.

Results. A significant difference was observed in the mean ADC value of the normal renal parenchyma and ccRCC – $1.82 \pm 0.16 \times 10^{-3} \text{ mm}^2/\text{s}$ vs $2.15 \pm 0.12 \times 10^{-3} \text{ mm}^2/\text{s}$, respectively ($p < 0,05$). Additionally, statistically reliable differences in ADC values in patients with high and low ccRCC grades were obtained: in patients with the I grade, the mean ADC value was $1.92 \pm 0.12 \times 10^{-3} \text{ mm}^2/\text{s}$, in patients with the II grade, this value was $1.84 \pm 0.14 \times 10^{-3} \text{ mm}^2/\text{s}$, in patients with the III grade, the mean ADC value was $1.79 \pm 0.12 \times 10^{-3} \text{ mm}^2/\text{s}$, and in patients with the IV grade of nuclear polymorphism the mean ADC value was $1.72 \pm 0.11 \times 10^{-3} \text{ mm}^2/\text{s}$ ($p < 0,05$).

Conclusions. The data obtained in the survey show a significant restriction in the diffusion of hydrogen molecules in tissues of ccRCC, compared to the healthy renal parenchyma due to the tumour's greater density. A statistically significant difference was observed in the mean ADC values of ccRCC tumours with different Fuhrman nuclear grades: tumours with a low grade of differentiation demonstrated higher mean ADC values compared to highly differentiated tumours. Application of DWI modality of MR imaging with ADC calculation allows to obtain valuable information that is vital for the diagnosis of ccRCC and differentiation of its degree of malignancy.

Key words

renal cell carcinoma, magnetic resonance imaging, diffusion-weighted imaging, apparent diffusion coefficient

Abbreviations

ADC – apparent diffusion coefficient; ccRCC – clear cell renal cell carcinoma; CT – computed tomography; DWI – diffusion-weighted images; FIESTA FAT SAT – fast imaging employing steady-state acquisition with fat saturation; FRFSE – fast-recovery fast spin-echo; FSPGR-DE – fast spoiled gradient-recalled echo dual-echo; LAVA – liver acquisition with volume acquisition; MRI – magnetic resonance imaging; RCC – renal cell carcinoma; ROI – region of interest; SNR – signal-to-noise ratio; SSFSE – single-shot fast spin-echo; TE – echo time; TR – repetition time

INTRODUCTION

Renal cell carcinoma (RCC) accounts for about 3% of malignant tumours of the adult population. In oncurology, this type of tumour ranks third after prostate and bladder cancer [1]. According to the American National Cancer Institute, for the past 20 years the incidence of RCC in the American population has been growing steadily and

accounts for 3.8% of all newly-diagnosed cancers, and the number of new cases expected in 2014 is approximately 70,000. At the same time, the mortality rate from this disease remains unchanged at 3.9%. Analysis of these indicators in recent years provides evidence that the incidence and mortality in patients with RCC is increasing steadily, despite the widespread use of modern methods of diagnosis and treatment (Fig. 1) [2].

Among various histological subtypes of RCC, the clear-cell subtype (ccRCC) is the most common and appears in 70–80% of pathological conclusions [3]. The degree of malignancy of ccRCC is determined on the background of various histological classifications, the Fuhrman grading

Address for correspondence: Andrzej Górecki, ZOZ Nr. 2, ul. Fredry 9, Rzeszów, Poland
E-mail: agorecki@mp.pl

Received: 26 February 2015; accepted: 12 May 2015

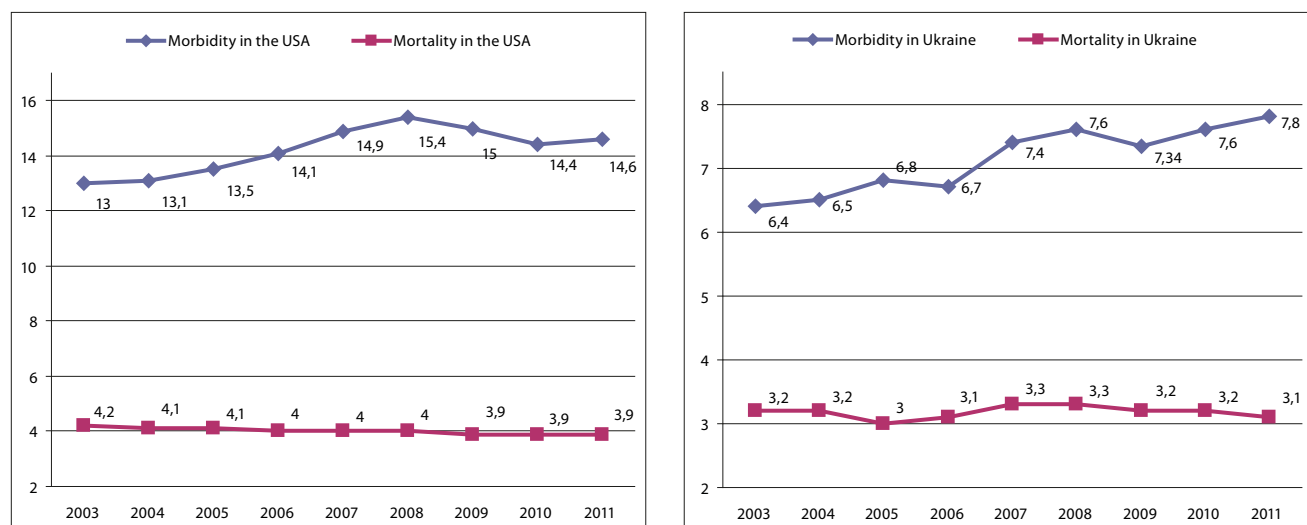


Figure 1. Dynamics of morbidity and mortality in patients with RCC in the USA and Ukraine during 2003–2011

system being the most commonly used, which is based on four morphologic criteria of the nuclei. Together with significant progress in understanding the mechanisms of RCC, an active survival option in selected patients was suggested; specifically, the degree of malignancy is a major criterion in the decision-making process regarding treatment options [4, 5].

Recently, computed tomography (CT) has been considered the 'gold standard' in diagnostic imaging of RCC, allowing the accurate staging of tumours, and determining the nature of their growth and detection of the presence of necrotic areas. Researchers have achieved promising results in the differentiation of histological subtypes of RCC and tumours with various degrees of nuclear atypia [6, 7]. However, the use of CT is always associated with radiation exposure and consequently carries a significant increase in the risk of malignancy in patients with aplastic processes [8, 9]. In recent years, MRI has increasingly attracted the attention of clinicians as the method of choice for the diagnosis and staging of RCC, due to several advantages over CT: excellent image quality, high information content, absence of any radiation exposure to patients and staff, ability to obtain three-dimensional images, assessment of renal function using contrast, etc. According to studies of the sensitivity and specificity of MRI with contrast enhancement in the differential diagnosis of RCC, it is quite comparable by these parameters to CT [10, 11].

The application of DWI representing the MRI modality which uses strong bipolar gradients to enhance sensitivity to thermally-induced Brownian motion of hydrogen molecules, allows the measurement of molecular diffusion in tissues *in vivo*. To date, DWI is used mainly for differential diagnosis of tumours of the central nervous system, but in recent years encouraging data has been received on the use of this technique in the diagnosis of diseases of other organs, including the kidneys. ADC is a quantitative parameter calculated from DWI images, which is used as a measure of diffusion in healthy and affected tissues [12, 13, 14].

Given the above, assessment of the efficacy of DWI modality of MRI and subsequent measurement of ADC in order to determine the parameters of the tumour and the degree of its differentiation in RCC is a vitally important issue.

OBJECTIVE

The purpose of the study was to assess the information content of MRI using DWI modality in the diagnosis of ccRCC. and determining the degree of its differentiation.

MATERIALS AND METHOD

Patients. A retrospective study was conducted among 62 adult patients with ccRCC tumours (32 men and 30 women), aged 42–73 years (mean age: 59.5 ± 1.2 years). The control group consisted of 15 healthy volunteers with no renal disease according to clinical and radiological examinations (9 men and 6 women) aged 23 – 46 years (mean age: 22.2 ± 1.8 years). The study exclusively involved patients with clear cell histological subtype of RCC. Patients with renal insufficiency, metal objects in the body, low image quality, and DWI with obvious artifacts were excluded from the study. All patients with ccRCC had undergone partial or radical nephrectomy with subsequent pathological verification of the diagnosis. According to the grading system of nuclear polymorphism in ccRCC, according to Fuhrman, patients were randomized as follows: I grade – 12 patients, II grade – 18 patients, III grade – 21 patients, and IV grade – 11 patients. Anticancer therapy in patients prior to the MRI and surgical treatment was not performed.

Research was approved by local Ethics Committee and conducted in clinics of the Department of Urology and Department of Radiology and Radiation Medicine of the National Medical University in L'viv, Ukraine, named after Danylo Halytsky, and at the 'Euroclinic' Medical Centre during 2013–2014.

MR Imaging Protocol. All patients with RCC and healthy volunteers underwent MRI, which included DWI, followed by ADC measurement. MR imaging was performed with a 1.5 T body scanner (Signa HDxt, General Electric, USA) using an eight-channel phased-array body coil. MR Imaging Protocol for renal masses included the following series: coronal T2-weighted single-shot fast spin-echo (SSFSE), breath-hold; axial 2D fast imaging employing steady-state acquisition with fat saturation (FIESTA FAT SAT); axial

DWI with b -values=0 and 800 mm^2/s , DWI was conducted prior to the administration of contrast media, using single-shot echo-planar imaging sequence with parallel imaging technique and fat saturation during one breath-hold; axial T1-weighted fast spoiled gradient-recalled echo dual-echo (FSPGR-DE), breath-hold; axial T2-weighted fast-recovery fast spin-echo (FRFSE); sagittal T2-weighted SSFSE; axial 3D fat-saturated T1-weighted spoiled gradient echo liver acquisition with volume acquisition (LAVA) during, and following administration of gadopentetate dimeglumine, in a dose of 0.1 mmol/kg of body weight as a bolus injection with 20 sec between each breath-hold acquisition.

Image Analysis. The signal intensity of the tumours on DWI was classified as high, iso- and low-signal intensity when compared with contralateral parenchyma. A colour ADC map was generated automatically at the workstation (Advantage Windows, GE Healthcare). The ADC was calculated using linear regression analysis of the function:

$$S = S_0 * \exp(-b * ADC)$$

where S is the signal intensity after application of the diffusion gradient, and S_0 is the signal intensity on the DW image acquired at $b=0 \text{ sec/mm}^2$.

The region of interest (ROI) was placed within a portion of the solid area, where the minimum ADC value on the ADC map was registered according to the colour by visual inspection. An average of 2–3 measurements per lesion were performed, depending on the lesion size. Necrotic regions were identified with conventional MRI sequences and were avoided for ROI placement. For comparison, the ROI placed in the tumour was copied and then placed on the normal parenchyma of the contralateral kidney in the same site in relation to the tumour, and in the corresponding upper or lower pole if the tumour produced a remarkable bulge outside the contour of the kidney. The mean ADC value was recorded within the ROI [15].

Statistical analysis. Functool software was used for ADC map generation and measurements, and SPSS 22.0 software was used for data processing. Descriptive statistical methods (mean, standard deviation) were used. The ADC values of cases were reported as the mean \pm standard deviation. Student's t -test was performed to compare the ADC values. Statistical significance was considered when P value was <0.05 .

RESULTS

Tumours had a predominantly irregular shape on MRI images with irregular and indistinct outlines. All tumours had a diameter exceeding 3 cm, with a mean size of $5.6 \pm 2.2 \text{ cm}$ (range from 3.0–13.5 cm). All patients had monofocal tumours. Patients with ccRCC in 49 (79%) cases demonstrated a homogeneous signal; the remaining 13 patients (21%) had a pronounced heterogeneous signal due to the presence of a necrotic component to the tumour. On MRI images, ccRCC was characterized by a hyperintense signal with regard to renal parenchyma on T2-weighted images, and a hypointense signal on T1-weighted images. On DWI, the tumour area was always represented by a hyperintense signal, while on the ADC-maps a corresponding zone appeared to be hypointense, compared to the unaffected renal parenchyma.

The performed analysis revealed that the average ADC value of malignant tumours was significantly lower compared to normal renal parenchyma and was $1.82 \pm 0.16 \times 10^{-3} \text{ mm}^2/\text{s}$ vs $2.15 \pm 0.12 \times 10^{-3} \text{ mm}^2/\text{s}$, respectively ($p < 0.05$), due to the significantly higher density of the ccRCC tissue, and consequently due to the limitation of the diffusion of hydrogen molecules within the tumour.

Evaluation of the mean ADC value in patients with different degrees of ccRCC malignancy in accordance with Fuhrman classification revealed a decrease in the mean ADC value, together with an increase of the nuclear polymorphism (Tab. 1). Statistical comparison of the patient data obtained from all 4 groups with different degrees of ccRCC differentiation, revealed a significant difference ($p < 0.05$) (Tab. 2). This data suggests that tumours with a higher degree of malignancy are characterized by a restriction in the diffusion of hydrogen molecules in their tissue on DWI.

Table 1. Mean ADC values of normal renal parenchyma and ccRCC

Pathologic type/stage (cases)	Mean ADC value ($\times 10^{-3} \text{ mm}^2/\text{s}$)
Normal renal parenchyma (n=15)	2.15 ± 0.12
ccRCC (n=62)	1.82 ± 0.16
Grade I (n=12)	1.92 ± 0.12
Grade II (n=18)	1.84 ± 0.14
Grade III (n=21)	1.79 ± 0.12
Grade IV (n=11)	1.72 ± 0.11

Table 2. Comparative analysis of the ADC value between normal renal parenchyma and ccRCC, and between tumours with different grades of differentiation

Comparison	P Value
ccRCC vs normal renal parenchyma	<0.05
ccRCC grade I vs ccRCC grade II	<0.05
ccRCC grade I vs ccRCC grade III	<0.05
ccRCC grade I vs ccRCC grade IV	<0.05
ccRCC grade II vs ccRCC grade III	<0.05
ccRCC grade II vs ccRCC grade IV	<0.05
ccRCC grade III vs ccRCC grade IV	<0.05

DISCUSSION

Recent studies have shown the importance of the DWI MR with subsequent ADC measurement in the diagnosis of the RCC [15, 16, 17, 18, 19, 20, 21, 22, 23, 24, 25].

In the presented study, a statistically significant difference was observed between the mean ADC values of the normal renal parenchyma and ccRCC tumours: $2.15 \pm 0.12 \times 10^{-3} \text{ mm}^2/\text{s}$ vs $1.82 \pm 0.16 \times 10^{-3} \text{ mm}^2/\text{s}$, respectively. The above data correlates with the results obtained by other scientists: Wang et al. used the 3T MR imaging system and b values 0 and 800, the mean ADC values of the normal renal parenchyma and ccRCC were $1.69 \pm 0.32 \times 10^{-3} \text{ mm}^2/\text{s}$ and $2.30 \pm 0.17 \times 10^{-3} \text{ mm}^2/\text{s}$, respectively [16]. In the presented study, the 1.5T imaging system was used which might explain some differences in the obtained data between the studies.

In another study, Razek et al. analyzed the ADC levels of the ccRCCs scanned on the 1.5T MR system with b values 0 and 800, and obtained results comparable to those of

the current study: the mean ADC value of the malignant tumors was $1.72 \pm 0.12 \times 10^{-3} \text{ mm}^2/\text{s}$. Additionally, the authors compared ADC levels of the other histological subtypes of the RCC and received a significant difference. Unfortunately, this study lacks the data on the mean ADC levels of the healthy kidney parenchyma [17].

Accurate characterization of the grades of differentiation of the ccRCC is essential for the prognosis and treatment tactics. The degree of malignancy of ccRCC is determined using various histological classifications. Currently, the 4-tiered Fuhrman grading system is most commonly used for defining the degree of differentiation of ccRCC. In a few recent studies, attempts were made to simplify this classification into a 3-tiered or even 2-tiered system [18, 19]. Sandrasegaran et al. in their work used the 2-tiered gradation system for the ccRCC. As a result of the ADC data analysis from patients with ccRCC (1.5T MR system and DWI with b values 0 and 800 were used), the authors achieved a difference in the ADCs of the low-grade and hi-grade tumours. The mean ADC value of the low-grade tumors was higher than in hi-grade lesions: $1.95 \pm 0.25 \times 10^{-3} \text{ mm}^2/\text{s}$ vs $1.77 \pm 0.20 \times 10^{-3} \text{ mm}^2/\text{s}$, respectively. However, the results were statistically unreliable [20].

In the presented study, the traditional 4-tier Fuhrman grading system was used and the results obtained had a similar trend to the above-mentioned study. Low differentiated ccRCCs (grades I and II) had the highest ADC values in comparison with low differentiated (grade III and IV) lesions: the mean ADC value of the I grade tumours was $1.92 \pm 0.12 \times 10^{-3} \text{ mm}^2/\text{s}$, this value was $1.84 \pm 0.14 \times 10^{-3} \text{ mm}^2/\text{s}$ in the II grade tumours, the mean ADC value was $1.79 \pm 0.12 \times 10^{-3} \text{ mm}^2/\text{s}$ in the III grade lesions, and in patients with the IV grade of ccRCCs, the mean ADC value was $1.72 \pm 0.11 \times 10^{-3} \text{ mm}^2/\text{s}$. The obtained data was statistically significant ($p < 0.05$).

The divergence in the mean ADC values in both studies can be explained by different methodology of the ROI placement. In the presented study, ROI was placed exclusively within a portion of the solid area, where the minimum ADC value on the ADC map was registered according to the colour by visual examination. In this study, 4–6 oval ROIs were placed over the renal masses on the ADC maps. These ROIs included as much of the tumour mass as possible while excluding the normal kidney parenchyma. In addition, small ROIs with a minimum area of 1–2 cm were placed along the centre and periphery of the mass.

In another study, Rosenkrantz et al. also exploited the 2-tier histologic gradation system of ccRCC, the DWI MR scanning was performed with the same parameters used in the current. A statistically significant difference was obtained in the mean ADC values of the low- and hi-grade tumours: $1.85 \pm 0.40 \times 10^{-3} \text{ mm}^2/\text{s}$ and $1.28 \pm 0.48 \times 10^{-3}$, respectively ($p < 0.001$). For this measurement, the mean ADC was recorded within a round ROI placed on the ADC map within a portion of the tumour showing visually low ADC [21]. The data obtained in this study corresponds to that demonstrated in the presented study.

Obviously, the current study has some limitations: the ADC values of other histologic subtypes of the RCC and of the malignant cysts should be analyzed in order to create a full-scale algorithm of the RCC differential diagnosis.

CONCLUSIONS

1. The data obtained in the study show a significant restriction of hydrogen molecules diffusion in tissues of ccRCC compared to the healthy renal parenchyma due to the greater density of the tumour.
2. Mean ADC value of the normal renal parenchyma was significantly higher than in ccRCC tissues, and was $2.15 \pm 0.12 \times 10^{-3} \text{ mm}^2/\text{s}$ and $1.82 \pm 0.16 \times 10^{-3} \text{ mm}^2/\text{s}$, respectively ($p < 0.05$).
3. A statistically significant difference was observed in the mean ADC values of ccRCC tumours with different degrees of nuclear atypia by Fuhrman: tumours with a low grade of differentiation demonstrated higher mean ADC value compared to highly differentiated tumours.
4. Application of DWI modality of MR imaging with ADC calculation the obtaining of valuable information that is vital for the diagnosis of ccRCC and differentiation of its degree of malignancy.
5. Further research is vitally important in order to establish the difference in the ADC values of the other histological subtypes of RCC and benign tumours of the kidney.

Note

The authors did not receive any funding for the research.

Competing interests

The authors declare that they have no competing interests.

REFERENCES

1. Jemal A, Siegel R, Ward E, et al. Cancer statistics. *A Cancer Journal for Clinicians* 2009; 59(4): 225–249.
2. Sun MR, Ngo L, Genega EM, et al. Renal cell carcinoma: dynamic contrast-enhanced MR imaging for differentiation of tumor subtypes – correlation with pathologic findings. *Radiology* 2009; 250: 793–802.
3. Eble JL, Sauter G, Epstein JI, et al. Pathology and genetics of tumours of the urinary system and male genital organs. Lyon: IARC; 2004.
4. Chevillon JC, Lohse CM, Zincke H, et al. Comparisons of outcome and prognostic features among histologic subtypes of renal cell carcinoma. *American Journal of Surgical Pathology* 2003;27(5):612–624.
5. Crepel M, Jeldres C, Perrotte P, et al. Nephron-sparing surgery is equally effective to radical nephrectomy for T1BN0M0 renal cell carcinoma: a population-based assessment. *Urology* 2010;75(2):271–275.
6. Miguel V, Fernando L, Carlos M, et al. Nuclear grade prediction of renal cell carcinoma using contrasted computed tomography. *J Urol*. 2009; 181(4): 249–249.
7. Sheir KZ, El-Azab M, Mosbah A, et al. Differentiation of renal cell carcinoma subtypes by multislice computerized tomography. *J Urol*. 2005; 174(2): 451–455.
8. Sodickson A. CT radiation risks coming into clearer focus. *BMJ*. 2013; 21: 346:f3102.
9. Mathews J, Forsythe A, Brady Z, et al. Cancer risk in 680 000 people exposed to computed tomography scans in childhood or adolescence: data linkage study of 11 million Australians. *BMJ* 2013; 346: f2360.
10. Kim JK, Kim TK, Ahn HJ, Kim CS, Kim KR, Cho KS. Differentiation of subtypes of renal cell carcinoma on helical CT scans. *AJR Am J Roentgenol*. 2002; 178: 1499.
11. Taouli B, Thakur R, Mannelli L. Renal Lesions: Characterization with Diffusion-weighted Imaging versus Contrast-enhanced MR Imaging. *Radiology*. 2009; 251(2): 398–407.
12. Taouli B, Vilgrain V, Dumont E, et al. Evaluation of liver diffusion isotropy and characterization of focal hepatic lesions with two single-shot echoplanar MR imaging sequences: prospective study in 66 patients. *Radiology* 2003; 226(1): 71–78.
13. Pedrosa I, Sun MR, Spencer M, et al. MR imaging of renal masses: correlation with findings at surgery and pathologic analysis. *Radiographics* 2008; 28(4): 985–1003.

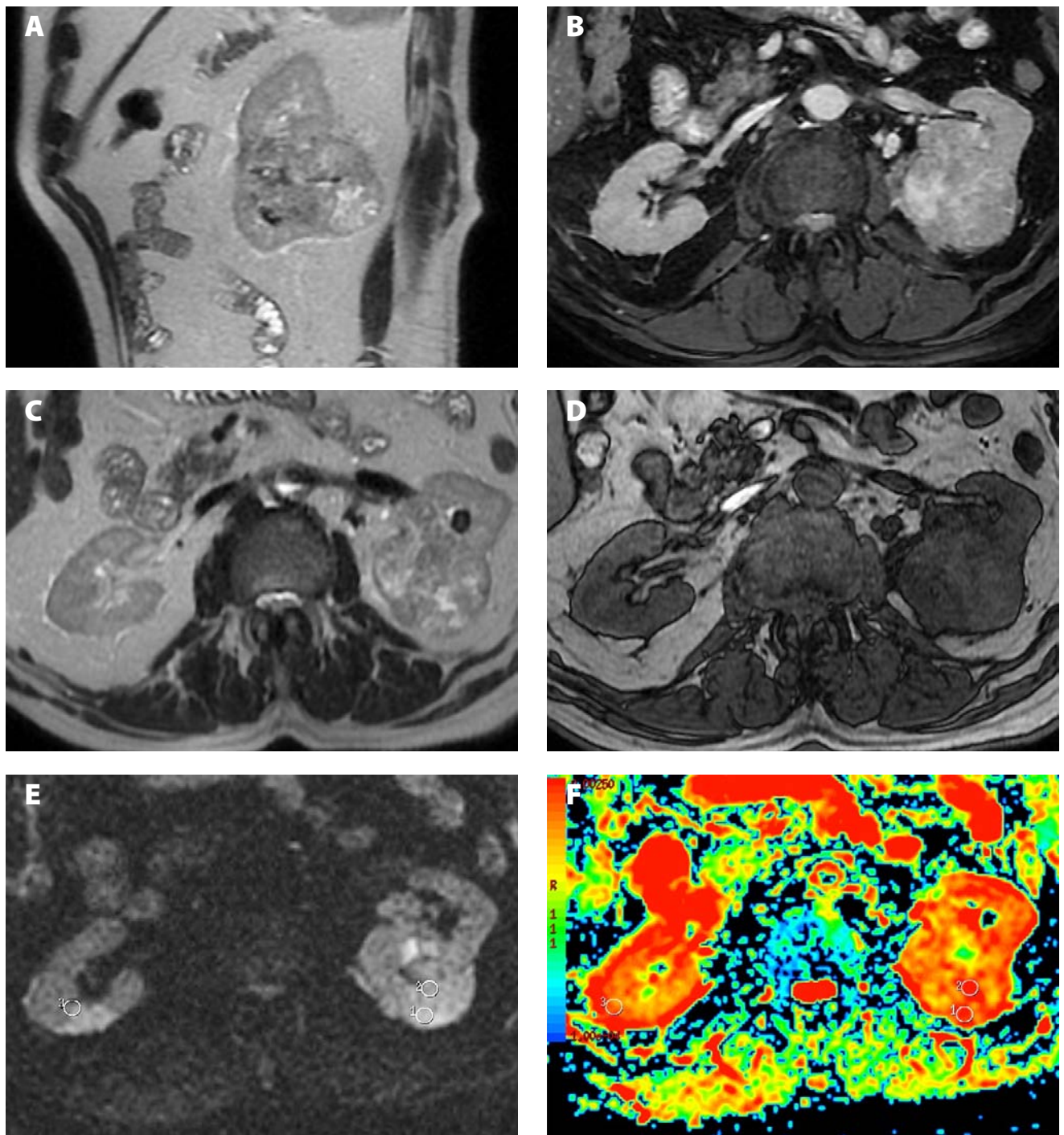


Figure 2. MRI of a patient, 74 y.o., confirmed by morphology ccRCC of the left kidney, III grade of differentiation by Fuhrman. A: on sagittal T2-weighted SSFSE a large tumour 68x75x55 mm with zones of iso- and hyper-intensity and without infiltration into surrounding tissues. B: on axial T2-weighted FIESTA with a fat saturation tumour is represented by regions of iso- and hyper-intensity. C: on axial T2-weighted SSFSE the regions of hyper-intensity over the tumour are well represented. D: on axial double-echo FSPGR the tumour is represented as iso- and hypointense regions. E: on axial DWI tumor is represented as a hyperintense region. F: ADC-map with b values 0 and 800, ROI1 and ROI2 over the tumour area showed the highest ADC values ($1.75 \times 10^{-3} \text{ mm}^2/\text{s}$ and $1.77 \times 10^{-3} \text{ mm}^2/\text{s}$), compared to ROI3 over the normal renal parenchyma of contralateral kidney ($2.16 \times 10^{-3} \text{ mm}^2/\text{s}$)

14. Sun MR, Ngo L, Genega EM, et al. Renal cell carcinoma: dynamic contrast-enhanced MR imaging for differentiation of tumor subtypes – correlation with pathologic findings. *Radiology* 2009; 250(3): 793–802.
15. Kumaresan S, Sundaram ChP, Ramaswamy R, et al. Usefulness of Diffusion-Weighted Imaging in the Evaluation of Renal Masses. *American Journal of Roentgenology* 2010; 194(2): 438-445.
16. Haiyi Wang, Liuquan Cheng, Xu Zhang, et al. Renal Cell Carcinoma: Diffusion-weighted MR Imaging for Subtype Differentiation at 3.0 T. *Radiology* 2010; 257(1): 135–143.
17. Razek AA, Farouk A, Mousa A, et al. Role of diffusion-weighted magnetic resonance imaging in characterization of renal tumors. *J Comput Assist Tomogr.* 2011;35(3): 332-336.
18. Sun M, Lughezzani G, Jeldres C, et al. A proposal for reclassification of the Fuhrman grading system in patients with clear cell renal cell carcinoma. *Eur Urol.* 2009; 56(5): 775-781.
19. Hong SK, Jeong CW, Park JH, Kim HS, Kwak C, Choe G, Kim HH, Lee, SE. Application of simplified Fuhrman grading system in clear-cell renal cell carcinoma. *BJU International* 2011; 107: 409–415.

20. Rosenkrantz B, Andrew , Benjamin E, Niver, Erin F, Fitzgerald, et al. Utility of the Apparent Diffusion Coefficient for Distinguishing Clear Cell Renal Cell Carcinoma of Low and High Nuclear Grade. *American Journal of Roentgenology* 2010; 195: 5: 344–351.
21. Le Bihan D. Molecular diffusion nuclear magnetic resonance imaging. *Magnetic Resonance Quarterly* 1991; 7(1): 1–30.
22. Hatakenaka M, Soeda H, Yabuuchi H, et al. Apparent diffusion coefficients of breast tumors: clinical application. *Magnetic Resonance in Medical Sciences* 2008; 7(1): 23–29.
23. Taouli B, Thakur RK, Mannelli L, et al. Renal lesions: characterization with diffusion-weighted imaging versus contrast-enhanced MR imaging. *Radiology* 2009; 251(2): 398–407.
24. Wang H, Cheng L, Zhang X, et al. Renal cell carcinoma: diffusion-weighted MR imaging for subtype differentiation at 3.0 T. *Radiology* 2010; 257(1): 135–143.
25. Cova M, Squillaci E, Stacul F, et al. Diffusion-weighted MRI in the evaluation of renal lesions: preliminary results. *British Journal of Radiology* 2004; 77(922): 851–857.